NASA CONTRACTOR REPORT NASA CR-132386

ELECTRON BEAM, LASER BEAM AND PLASMA ARC WELDING STUDIES

By

Conrad M. Banas

Prepared by

UNITED AIRCRAFT RESEARCH LABORATORIES
East Hartford, Conn.

for

NATIONAL AERONAUTICS AND SPACE ADMINISTRATION
LANGLEY RESEARCH CENTER

March 1974

N03-252-1

NASA CR-132386

ELECTRON BEAM, LASER BEAM AND PLASMA ARC WELDING STUDIES

By C. M. Banas

Prepared under Contract No. NAS1-12565 by
UNITED AIRCRAFT RESEARCH LABORATORIES
East Hartford, CT

for

NATIONAL AERONAUTICS AND SPACE ADMINISTRATION

FOREWORD

Electron beam, plasma arc and gas tungsten arc weld samples were prepared by Weld Development Laboratory (WDL) and Materials Engineering Research Laboratory (MERL) personnel of the Pratt and Whitney Aircraft Division of United Aircraft Corporation. These personnel also provided metallographic, NDI and mechanical property evaluations of the weld specimens. The assistance of these personnel, and, in particular, of D. Rutz and D. Anderson of MERL, in the performance of the subject program is gratefully acknowledged.

The NASA program monitor for this contract was D. M. Royster.

ELECTRON BEAM, LASER BEAM AND PLASMA ARC WELDING STUDIES

by C. M. Banas
United Aircraft Research Laboratories

SUMMARY

A direct comparison was made of electron beam, laser beam and arc welding processes in Ti-6Al-4V alloy in nominal thicknesses of 0.10, 0.15, 0.20 and 0.64 cm (0.04, 0.06, 0.08 and 0.25 in). Bead-on-plate penetrations were initially formed to establish optimum welding parameters for each process. A total of fifty-six butt welds approximately 12.7 cm in length were then prepared for detailed evaulation. Twenty-four specimens, two in each thickness by each welding process, were stress relieved in vacuum at 538°C for a period of two hours, radiographed and forwarded to the NASA Langley Research Center for examination. Thirty-two butt weld samples, four in each thickness by laser and two each by electron beam and arc processes, were stress relieved in air at 538°C for a period of two hours and subjected to metallographic, NDI and mechanical test.

Examination of the specimens showed that welds prepared by all processes were radiographically sound and exhibited tensile strengths (with bead reinforcement) equal to or greater than that of the base material. Electron beam and laser welds were formed at substantially lower energy inputs per unit weld length than either plasma arc or gas tungsten arc welds. For this reason the former experienced much more rapid cooling rates and therefore exhibited finer fusion zone grain structure than the latter. On the other hand, the rapid cooling rates encountered in electron and laser beam welds led to increased weld zone hardness and decreased fracture toughness in comparison to arc welds. Specifically, arc welds exhibited a fracture toughness only 10% below that of the parent material while beam welds showed a decrease of approximately 40%. It is evident that additional parameter development will be required for beam welds scheduled for applications requiring high fracture toughness and/or that more intensive post-weld processing will be required for such welds.

RECOMMENDATIONS

Based on the results of this program it is recommended that:

1. Investigations be conducted to establish electron and laser beam welding parameters leading to improved fracture toughness properties in Ti-6Al-4V welds. Consideration should also be given to modified post-weld heat treatment of beam welds in order to improve toughness characteristics.

2. Comparisons of electron beam, laser beam and plasma arc welding in Ti-6Al-4V alloy should be extended to include an evaluation of fatigue characteristics.

3. Comparisons of electron beam, laser beam and plasma arc welding should be extended to other important aerospace construction materials.

INTRODUCTION

Recent developments in high power laser welding (ref. 1) indicate that laser utilization for significant production welding tasks is near at hand. High speed laser welds with excellent metallographic, radiographic and mechanical properties have been demonstrated in a variety of materials. Simple gas shielding techniques have been employed to produce high quality welds in reactive metals. For example, as may be noted in fig. 1, laser welds exhibiting a broad range of fusion zone characteristics have been formed in titanium alloys. These encouraging results coupled with the unparalleled adaptability of laser welding to automation underscore the desirability for more comprehensive evaluation of the laser welding process.

Initial laser welding results, refs. 1-3, have generally been compared with other laser welding work. While this procedure has established the current capability of laser welding, information pertaining to the advantages and/or disadvantages of this process in comparison to established welding methods has been lacking. It was, therefore, deemed desirable to provide a direct comparison of laser beam welding with other advanced welding processes.

The program described herein was undertaken as an initial step in establishing an evaluation framework which would permit a priori selection of advanced welding processes for specific applications. To this end, a direct comparison of laser beam, electron beam and arc welding of Ti-6Al-4V alloy was undertaken. Ti-6Al-4V was selected for use in this study in view of its established welding characteristics and its importance in aerospace applications.

EXPERIMENTAL APPARATUS & PROCEDURE

Laser Facility

A 6 kW, CO_2 laser developed at the United Aircraft Research Laboratories was used for the tests conducted in this program. This system, shown in fig. 2, utilizes high volume gas flow to convectively cool the laser cavity and permit effective, continuous operation at multikilowatt power levels. Laser gases are cooled and recirculated in order to minimize system operational costs. An oscillator-amplifier unit provides a Gaussian output beam with near-diffraction-limited focusability.

For welding tests in this program a spherical focusing mirror having a nominal 76 cm focal length (f/11.5) was used. A nominal focused spot diameter of approximately 0.10 cm is customarily achieved with this focusing element providing a power density of approximately 7.6×10^5 W/cm^2 at 6 kW. The mirror was positioned to direct the focused beam downward onto a horizontal workpiece (downhand welding position). Inert gas shielding, as shown in fig. 3, protected the weld zone from the atmosphere. Typical flow rates for the combination of helium and argon gas were on the order of 300 cm^3/s.

Electron Beam and Arc Welding Equipment

The electron beam unit used was a 6 kW, Hamilton Standard Model W-2 welder. This unit provides a maximum output of 40 mA of electron beam current at an output voltage of 150 kV. Environmental protection for the welds is provided by the beam vacuum chamber.

Butt welds in 0.64 and 0.20 cm thick material were formed with an Airco Model PPT-200 plasma arc welder. Gas tungsten arc welds were made in 0.15 and 0.10 cm nominal thickness material with a P&H DCR-HFGW, 300 A unit.

Procedure

Weld specimens were chemically cleaned prior to welding in accordance with standard practice for titanium alloy weldments as noted, for example, in ref. 4. The specimens were 7.6 x 15.2 cm in size with the 15.2 cm edge machined square to provide good butt weld fit up; welded panels were 15.2 square with acceptable weld zones at least 12.7 cm in length. As noted in Table I, filler was utilized in all electron beam welds except one. The filler material used was 0.76 mm Ti-6Al-4V wire which was initially tack welded in place. Filler was also used in some plasma arc welds and in all gas tungsten arc welds; none was used in laser welds.

Initially, bead-on-plate penetrations were formed in order to establish optimum welding parameters. More than forty such penetrations were formed by laser; only limited tests were required with electron beam and plasma arc processes. It was found, however, that the available plasma arc equipment was not suitable for welds in the two thinner gages, gages for which the keyhole mode can not be utilized (ref. 5). Therefore, gas tungsten arc welds were substituted for plasma arc welds in nominal 0.10 and 0.15 cm thick material. It is felt that the similarity in GTA and plasma arc processes in the melt-in mode for these thicknesses permits this interchange without adversely influencing general comparisons.

Sample butt welds were stress relieved at 538°C for two hours. Weld specimens retained for test at United Aircraft Corporation were stress relieved in air. Samples forwarded to NASA Langley for evaluation were relieved in vacuum. Apart from the surface discoloration encountered during the stress relief in air, no differences would be anticipated from variance in environment for material of this thickness. All sample welds were radiographed and then subjected to further tests.

Hardness measurements were made with a Vickers unit using a 5 kg load. Tensile test information was obtained in accordance with ASTM specification E8. A 5.08 cm long gage length encompassing the transverse weld zone with bead reinforcement intact was used to determine elongation data. Elongation was measure in reference to scribe lines established along the gage length; no correction was made for the effective gage length change due to the presence of the less-ductile weld zone.

RESULTS

Welding Parameters

Optimized welding parameters for the electron beam, laser beam and arc welding processes used in this program are presented in Table I. It is to be noted that filler material was added in all electron beam welds, in the 0.20 cm plasma arc weld and in gas tungsten arc welds delivered to NASA Langley. No filler was used in laser welds, in the 0.64 cm plasma arc weld or in the high speed electron beam weld (4.23 cm/s) prepared in 0.15 cm thick material for more detailed comparison of laser and EB weld microstructure.

Optimum power levels were highest for laser welds and, therefore, provided the fastest welding speeds for the three processes investigated. Both electron beam and laser welding speeds were more than an order of magnitude faster than those for arc welds. Further, both electron beam and laser beam welds exhibited very low energy requirements per unit weld length, generally less than 25% of those for arc welding. Electron beam welds had the lowest specific weld energy requirements and generally exhibited the narrowest fusion zones.

Although the parameters noted in Table I were selected for this program, it is well to note that considerable flexibility exists in such choice for beam welds. In particular, reduction in welding speed is possible with both types of welding techniques such that an increase in specific welding energy occurs and a broader fusion zone can be obtained. This variation in electron beam welding is facilitated by use of circle spot generation. For laser welding, no beam oscillation appears necessary over a wide range of speeds; broader beads may also be facilitated by location of the workpiece surface at a position other than the beam focal point such that the power density incident on the surface is reduced.

Weld Evaluation

Visual Inspection.- Visual inspection of welds formed by all three processes revealed a bright; shiny bead appearance which indicated that shielding techniques were adequate to prevent atmospheric contamination. Weld beads were generally smooth in appearance with uniform soldification lines; some slight undercutting was noted in a few instances for which filler material was not utilized. The narrowest beads were formed by electron beam, somewhat broader zones were obtained with the laser and still broader zones occurred by the arc process.

Electron beam welds exhibited a marked degree of metal spatter on the lower weld surface. Although such spatter can be somewhat reduced by particular control of weld parameters, it is the consequence of the extremely high power density afforded by the electron beam and is often characteristic of welds formed by this process. It is anticipated that such spatter would be detrimental to fatigue endurance properties and therefore should be removed prior to weldment use in fatigue-critical applications. The somewhat lower power density characteristic of the laser beam essentially eliminates the weld spatter problem.

Radiography. - All butt weld samples were radiographed prior to delivery to NASA Langley. It was found that the weld zones were essentially free of defects over a length of at least 12.7 cm. Representative radiographs for 0.64 cm and 0.20 cm thick material are presented in figs. 4 and 5. Since run off tabs were not utilized, start and stop defects may be noted in most cases; such defects, however, did not influence weld characteristics within the acceptable weld length.

It is noted that the electron beam welds are quite narrow and exhibit a somewhat nonuniform radiographic appearance due to the lower surface weld spatter. Laser beam welds, as evidenced in figs. 4 and 5, exhibit an extremely uniform weld zone characteristic and a relatively narrow bead width. Arc welds are considerably broader but also quite uniform in density.

Exceptions to the general radiographic soundness of sample welds were encountered in 0.10 cm thick material welds formed by laser beam and gas tungsten arc which were delivered to NASA Langley for evaluation. The nature of the defects (a region of fine-grained porosity in GTA welds and sporadic holes in laser beam welds) indicated possible inadequate cleaning in the preparation of the GTA welds and a joint fit up problem in the case of the laser welds. Other GTA and laser welds prepared in 0.10 cm material prior to and subsequent to the delivery date for NASA Langley sample welds showed acceptable properties. It is therefore concluded that the noted defects were the result of inadequate weld preparation and not due to a shortcoming of either welding process.

Hardness.- The hardness of the base material, heat-affected zone and fusion zone was measured for all butt weld specimens and is presented in Table II. A Vickers diamond point hardness tester with a 5 kg load was used for these measurements. It was found that the Vickers hardness number for the base material varied from 293 - 362 with an average value of approximately 330.

It is noted with reference to Table II that the hardness of the heat-affected zone was only slightly higher than that of the base material for all welding processes. On the other hand, substantial increases in fusion zone hardness over that of the base material are noted, with the highest increases in hardness occurring in laser and electron beam welds. The maximum increase in hardness occurred in an electron beam weld formed in 0.15 cm thick material at a welding speed of 4.23 cm/s; the increase from base material hardness was of the order of 22%. This weld, as shown in Table I, was characterized by the lowest specific energy input of all welds examined, a specific weld energy of only 0.24 kJ/cm. This extremely low energy input apparently led to a very high cooling rate in this case with the resultant maximum increase in weld zone hardness.

Tensile Properties.- Results of tensile tests conducted on sample welds in accordance with ASTM specification E8 are shown in Table III. Here, it is noted that only one of the sample specimens prepared failed in the weld zone, namely the electron beam weld specimen in 0.64 cm thick material. Detailed examination of this tensile specimen revealed a slight undercut at the edge of the fusion zone at which point the fracture occurred. It should be noted, however, that the ultimate tensile strength of this weld was essentially equivalent to that for the base material although the ductility, as evidenced by the markedly reduced elongation, was substantially lower.

Metallographic Properties.-

Macrostructure: The macrostructure of representative laser, electron beam and plasma arc welds in 0.64 cm thick material is shown in fig. 6 and for 0.20 cm thick material in fig. 7. Reference to these figures shows that the extent of the fusion zone is substantially smaller for electron beam and laser welds than for arc welds and the characteristic grain size is correspondingly smaller. In particular, extremely fine grain structure is to be noted for the laser weld in 0.20 cm thick material shown in fig. 7. By comparison, grain structure in the plasma arc weld in this thickness is quite coarse with the grain size approaching the overall size of the laser weld fusion zone in some instances.

Another feature evident from examination of figs. 6 and 7 is the existence of a relatively planar weld bead centerline grain boundary in both electron beam and laser beam welds. Although this might appear to be a plane of weakness in the weld zone, the results of tensile test measurements show that this is, in fact, not the case.

Microstructure: Microstructure in the weld zones is shown in figs. 8 and 9. With reference to fig. 8, it is noted that laser and electron beam welds in 0.64 cm thick material exhibit a fine grain structure characteristic of a rapid cooling rate. The plasma arc weld shown in fig. 8 has a structure indicative of a slower cooling rate than that encountered in the beam welds.

In 0.20 cm thick material, fig. 9, laser and electron beam welds again exhibit structures indicative of a more rapid cooling rate than plasma arc welds. In the two thinner gages, all welds exhibit structures characteristic of a very rapid cooling rate. The finest structure was observed in the electron beam weld prepared in 0.15 cm thick material at a welding speed of 4.23 cm/s. It has previously been noted that this specimen was subjected to the lowest energy input per unit weld length of all the weld specimens examined and possessed the highest fusion zone hardness. These factors together with the fine grain structure attest that the most rapid cooling rate was encountered by this specimen.

Fracture Toughness Characteristics.- Slow bend fracture toughness measurements obtained in accordance with ASTM E399-T are listed in Table IV. As shown in Table IV, base material values for the stress intensity factor, K_Q, were of the order of $8 \times 10^7 (Pa)(cm)^{1/2}$. The factor is referred to as K_Q rather than K_C since the small specimen size permissible did not insure that pure, plane strain was encountered in all cases.

The welds examined, which had been subjected to a two hours stress relief at 538°C, all exhibited a lower fracture toughness than that of the base material. For plasma arc welds the reduction of fracture toughness was of the order of 10%, while both laser and electron beam welds exhibited reductions of the order of 40%. It is obvious that the post-weld stress relief used for beam welds was inadequate for conditions requiring high fracture toughness. It is noted that complete re-heat treatment of electron beam welded Ti-6Al-4V alloy has been utilized to achieve desirable fracture toughness properties; similar procedures may be required for laser beam welds as well.

DISCUSSION OF RESULTS

Comparison of the various metallographic and mechanical test properties of the sample welds indicates a general overall correlation. This fine, acicular alpha and beta structure in electron beam and laser beam welds evidences a much faster cooling rate than that for arc welds. It would therefore be anticipated that beam welds would exhibit a higher fusion zone hardness than arc welds; this expectation is borne out by the hardness evaluations. As might be expected, the electron beam weld formed at 4.23 cm/s in 0.15 cm thick material exhibited the finest grain structure and the maximum increase in hardness.

A principal factor influencing the cooling rate is the weld energy input per unit length, with low values indicating correspondingly more rapid temperature decrease following welding. This behavior is quite evident in the comparison of arc welds with laser beam welds and in the comparison of electron beam welds with arc welds. An apparent anomaly in this relationship exists, however, in hardness comparisons of electron beam and laser welds. Reference to Tables I and II indicates that most laser welds are harder than comparable electron beam welds in material of the same thickness even though the weld energy input per unit length is somewhat higher for the former process. It should be noted, however, that the laser welds were formed in an atmospheric pressure environment with effective forced convection cooling afforded by the flow of inert shielding gas over the weld surface. It is apparent that the influence of convective cooling on the weld zone is not negligible in comparison to that in the vacuum environment of the electron beam. Further, it is possible that some of the incident laser energy may be reflected rather than absorbed by the workpiece. Information contained in ref. 6, however, indicates that such reflection is less than 10% for titanium. It is therefore concluded, as evidenced by the increased hardness in the laser weld zone, that more rapid cooling rates were experienced by laser welds in spite of slightly higher energy input. This behavior was observed for comparisons in which laser specific energy input was a factor of two or less greater than that for the electron beam. For 0.15 cm thick material, for which the energy input per unit length of laser weld was approximately 3.4 times that for the comparable electron beam weld, the latter exhibited the greater hardness and should be concluded to have experienced the more rapid cooling rate. In this case it can be reasoned that the effects of convective cooling were insufficient to offset the increased energy used for the laser weld. The extremely fine grain structure of the electron beam weld also attests a high cooling rate.

The tensile properties of the welds are in agreement with prior

experience for Ti-6Al-4V and are indicative of the strengthening due to hardening. Slow bend fracture toughness test results for weld material are also in relative agreement with the results of metallographic analysis and hardness measurements. The effect of microstructure on fracture toughness has been previously determined for several alloys (refs. 5,7) and alpha-phase morphology and distribution have been found to play a dominant role in determining this property. Toughness is optimized when alpha platelet thickness (ref. 7) is large enough to cause deflection of a propagating crack, while platelet length is short enough and platelet spacing is close enough to cause frequent changes in crack growth direction. Very fine acicular alpha structures, as were observed in both the laser and electron beam weld fusion zones, lead to relatively-long, uninterrupted alpha-beta interfaces along which cracks can readily propagate. Conversely, plasma arc weld fusion zones exhibited a Widmanstatten microstructure and therefore the resultant fracture toughness was closer to that of the base material. It should be noted, however, that the fracture toughness specimens were taken from welds formed in 0.64 cm thick material. Since the weld zones in the thinner gages all exhibited acicular structures, it may be anticipated that substantial reductions in fracture toughness occurred for arc welds in these thinner materials as well as for beam welds.

In general, the beam welding processes can be considered as low specific energy input, high speed processes while the arc processes involve substantially higher specific energy inputs and slower welding speeds. The latter processes have been shown to produce satisfactory tensile and fracture toughness properties after only a two hour stress relief at 538°C. Conversely, low energy input welds subjected to the same stress relief exhibit a low fracture toughness stemming from the higher cooling rates experienced by the weld material. Beam welds, however, exhibit excellent tensile properties and fine grain structure.

For applications requiring increased fracture toughness, electron beam and laser beam welding conditions leading to higher specific energy input (and therefore to slower cooling rates) or modified post-weld heat treatment can be utilized. For electron beam welding, the former may be accomplished by means of oscillating the beam spot such that a reduction in effective power density is obtained; the Hamilton Standard welder used in this program has a circle generator for this purpose. In laser beam welding, as evidenced by the cross sections shown in fig. 1, substantial flexibility exists in selection of welding speed at fixed power level with resultant marked variation in specific weld energy. Further increase in specific weld energy may be obtained by locating the surface of the workpiece away from the point of maximum focus, i.e., by reducing the incident beam power density. It should be noted that

the procedure discussed here will, as the result of the increase in specific weld energy, reduce welding speed at constant power level and also cause increased grain size. It is evident that selection of weld parameters must be tempered by application requirements. Extension of the present comparison of advanced welding processes to include fatigue endurance properties therefore appears warranted.

An alternative approach to attainment of improved fracture toughness in electron beam and laser beam welds might lie in utilization of a higher temperature (greater than 538°C) post-weld heat treatment. Two possible approaches which might be investigated are: 1) a full re-heat treatment of the material and 2) utilization of an 593-771°C overaging cycle.

SUMMARY OF RESULTS

1. Radiographically sound welds were formed in Ti-6Al-4V alloy by electron beam, laser beam and arc welding processes.

2. The tensile properties of laser, electron beam and arc welds subjected to a post-weld stress relief of two hours at 538°C exceeded base material levels in all but one specimen; the latter exhibited an ultimate tensile strength essentially equal to that of the base material.

3. The fracture toughness of all welds formed was lower than that of the base material. Plasma arc welds exhibited a toughness reduction of approximately 10% over that of the base material while the reduction for beam welds was of the order of 40%.

4. The weld energy per unit length for laser and electron beam welds was substantially lower than for arc welds. The lower specific energy input led to more rapid cooling in beam welds and therefore to a harder and finer-grained weld structure.

5. General overall correlation was obtained among results of metallographic, energy input, hardness and mechanical test observations. An apparent anomaly relative to hardness and specific energy comparisons in electron beam and laser welds was attributed to the influence of convective cooling on laser welds.

REFERENCES

1. Banas, C. M.: Laser Welding Developments. Paper presented at the CEGB International Conference on Welding Related to Power Plants (Southampton, England), Sept. 17-21, 1972.

2. Locke, E; Hoag, E.; and Hella, R.: Deep Penetration Welding with High Power CO_2 Lasers. Welding Journal, vol. 51, no. 5, May 1972, pp. 245s-249s.

3. Baardsen, E. L.; Schmatz, D. J.; and Bisaro, R. E.: High Speed Welding of Sheet Steel with a CO_2 Laser. Welding Journal, vol. 52, no. 4, April 1973, pp. 227-229.

4. Griffing, L., ed.: Welding Handbook. Section Four-Metals and Their Weldabiltiy. Sixth ed., American Welding Society, 1972.

5. Greenfield, M. A.; and Margolin, H.: The Interrelationship of Fracture Toughness and Microstructure in a Ti-5.25 Al-5.5V-0.9Fe-0.5Cu Alloy. Met. Trans., vol. 2, 1971, p. 841.

6. Seaman, F. D.: Establishment of a Continuous Wave Laser Welding Process. Report IR-809-3 (2) (Air Force Contract F33615-73-C-5004), Sciaky Bros., Inc., Jan. 1974.

7. Hall, J. A.; Pierce, C. M.; Ruckle, D. L.; and Sprague, R. A.: Property-Microstructure Relationships in the Ti-6Al-2Sn-4Zr-6 Mo Alloy. Materials Science and Engineering, vol. 9, 1972, p. 197.

TABLE I
SELECTED WELDING PARAMETERS
Ti-6Al-4V

Process	Power, kW	Weld Speed, cm/s	Specific Weld Energy, kJ/cm
0.64 cm nominal thickness material			
Electron Beam*	1.61	1.27	1.27
Laser	5.50	2.12	2.59
Plasma Arc	2.10	0.19	11.05
0.20 cm nominal thickness material			
Electron Beam*	1.17	1.69	0.69
Laser	5.50	5.93	0.93
Plasma Arc	0.50	0.12	4.17
Plasma Arc*	0.76	0.23	3.30
0.15 cm nominal thickness material			
Electron Beam*	0.91	1.69	0.69
Electron Beam	1.03	4.23	0.24
Laser	5.50	6.77	0.81
Gas Tungsten Arc*	1.60	0.16	10.00
0.10 cm nominal thickness material			
Electron Beam*	0.78	1.69	0.46
Laser	5.50	6.77	0.81
Gas Tungsten Arc	0.76	0.15	5.07

* Filler material added
For EB welds, 0.76 mm Ti-6Al-4V wire, tack welded in place, was used.

TABLE II

WELD ZONE HARDNESS CHARACTERISTICS
Ti-6Al-4V

Vickers Hardness, 5 kg Load

Process	Base Material	Heat-Affected Zone	Fusion Zone
0.64 cm nominal thickness material			
Electron Beam*	310-341	325-367	371-381
Laser	341	362	396
Plasma Arc	325-329	336	345-358
0.20 cm nominal thickness material			
Electron Beam*	317-321	306-336	362-386
Laser	329-336	336-345	381-391
Plasma Arc	341-362	358-367	367
Plasma Arc*	336-353	362-367	362-367
0.15 cm nominal thickness material			
Electron Beam*	329-341	336-341	391-401
Electron Beam	332-336	336	396-423
Laser	336	325-341	401
Gas Tungsten Arc*	341-345	367-376	376-381
0.10 cm nominal thickness material			
Electron Beam*	321-325	332-345	376-391
Laser	329	321-329	391-401
Gas Tungsten Arc*	293-299	321-362	362-386

* Filler material added

TABLE III

TENSILE STRENGTH CHARACTERISTICS
Ti-6Al-4V

Specimen*		Thickness, cm	0.2% Y.S., Pa 10^{-6}	U.T.S., Pa 10^{-6}	% Elongation 5.1 cm zone
Base Material	A	0.64	91.8	100.5	13.9
	B	0.64	92.1	101.9	12.1
	C	0.10	97.0	103.4	13.3
	D	0.10	98.4	103.4	13.3
Laser Weld	A	0.64	94.9	104.8	12.0
	B	0.64	94.6	103.7	11.6
	C	0.10	94.6	102.6	12.3
	D	0.10	94.6	101.9	12.0
EB Weld	A**	0.64	94.9	101.9	5.6
	B	0.64	94.9	103.0	9.6
	C	0.10	95.3	103.0	13.5
	D	0.10	94.6	103.0	13.6
Plasma Arc Weld	A	0.64	93.8	106.2	12.0
	B	0.64	94.8	106.2	10.0
GTA Weld	A	0.10	94.2	103.0	9.5
	B	0.10	93.5	102.6	10.3

* Specimens and test procedure in accordance with ASTM specification E8

** All weld tensile specimens failed in the base material with the exception of EB weld "A". This specimen exhibited a slightly undercut fusion zone at the point where the failure occurred.

TABLE IV

SLOW BEND FRACTURE TOUGHNESS CHARACTERISTICS
Ti-6Al-4V

Specimen*		Stress Intensity Factor, K_Q, Pa $(cm)^{1/2}$ x 10-3
Base Material	A	7.92
	B	8.10
	C	8.33
Laser Weld	A	5.16
	B	4.74
	C	4.69
EB Weld	A	4.47
	B	4.60
	C	4.90
Plasma Arc Weld	A	6.33
	B	6.62
	C	7.34

* Specimens and test procedure in accordance with ASTM specification E399-T

Specimens prepared from welds in 0.64 cm thick material

FIGURE 1. EFFECT OF SPEED ON LASER WELD CROSS SECTIONS

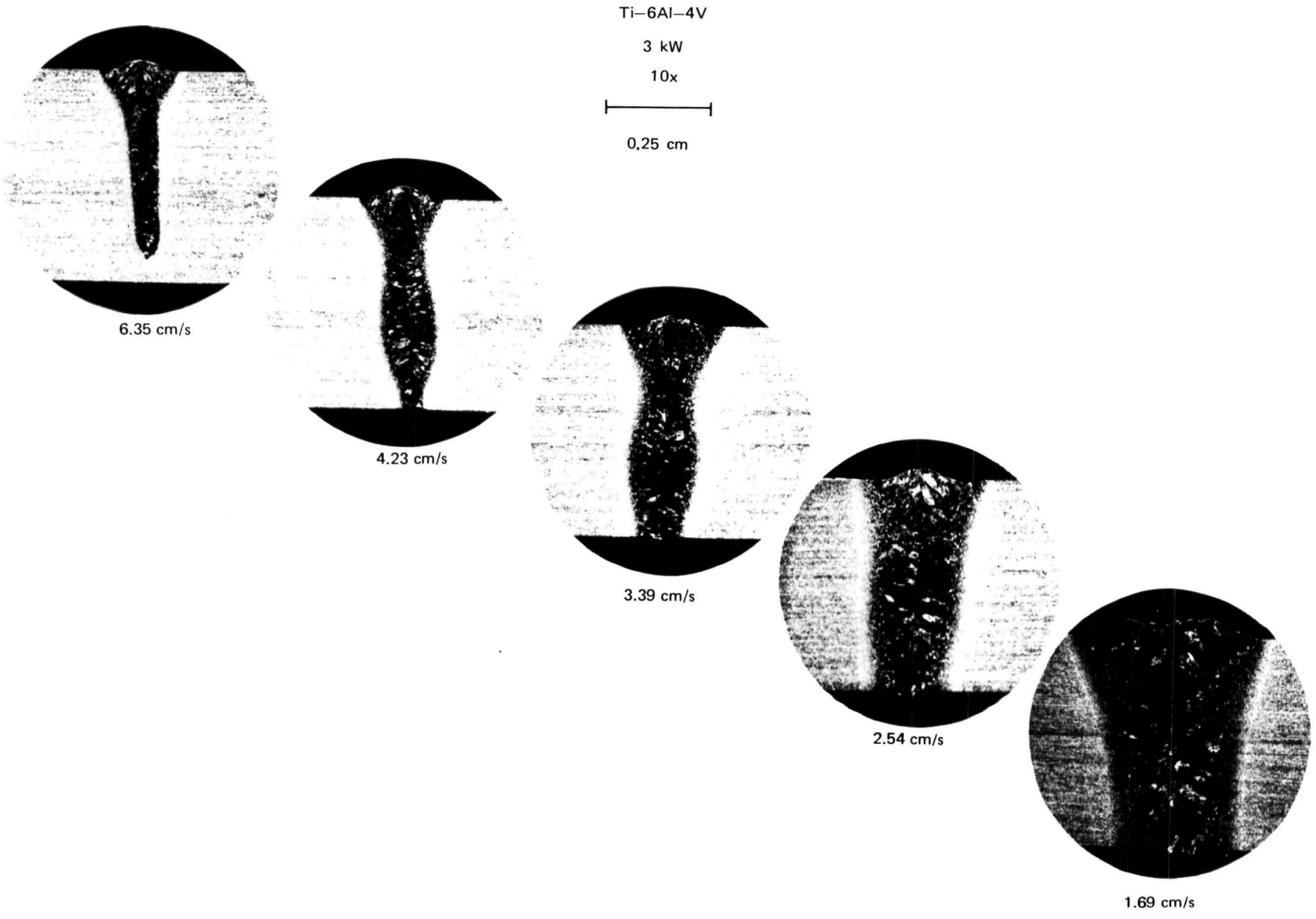

FIGURE 2. **6 kW LASER INSTALLATION**

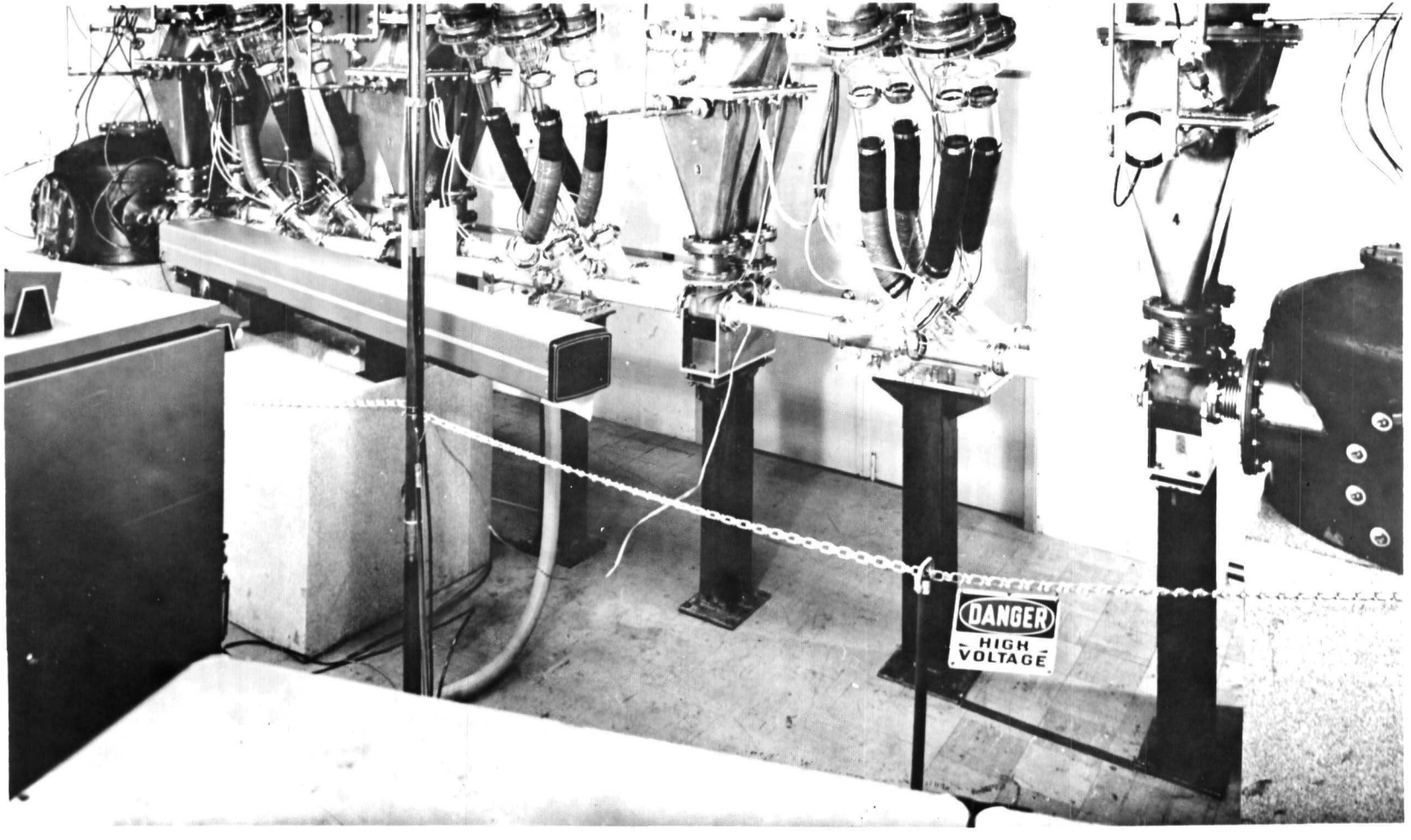

FIGURE 3. INERT GAS SHIELD WELD FIXTURE

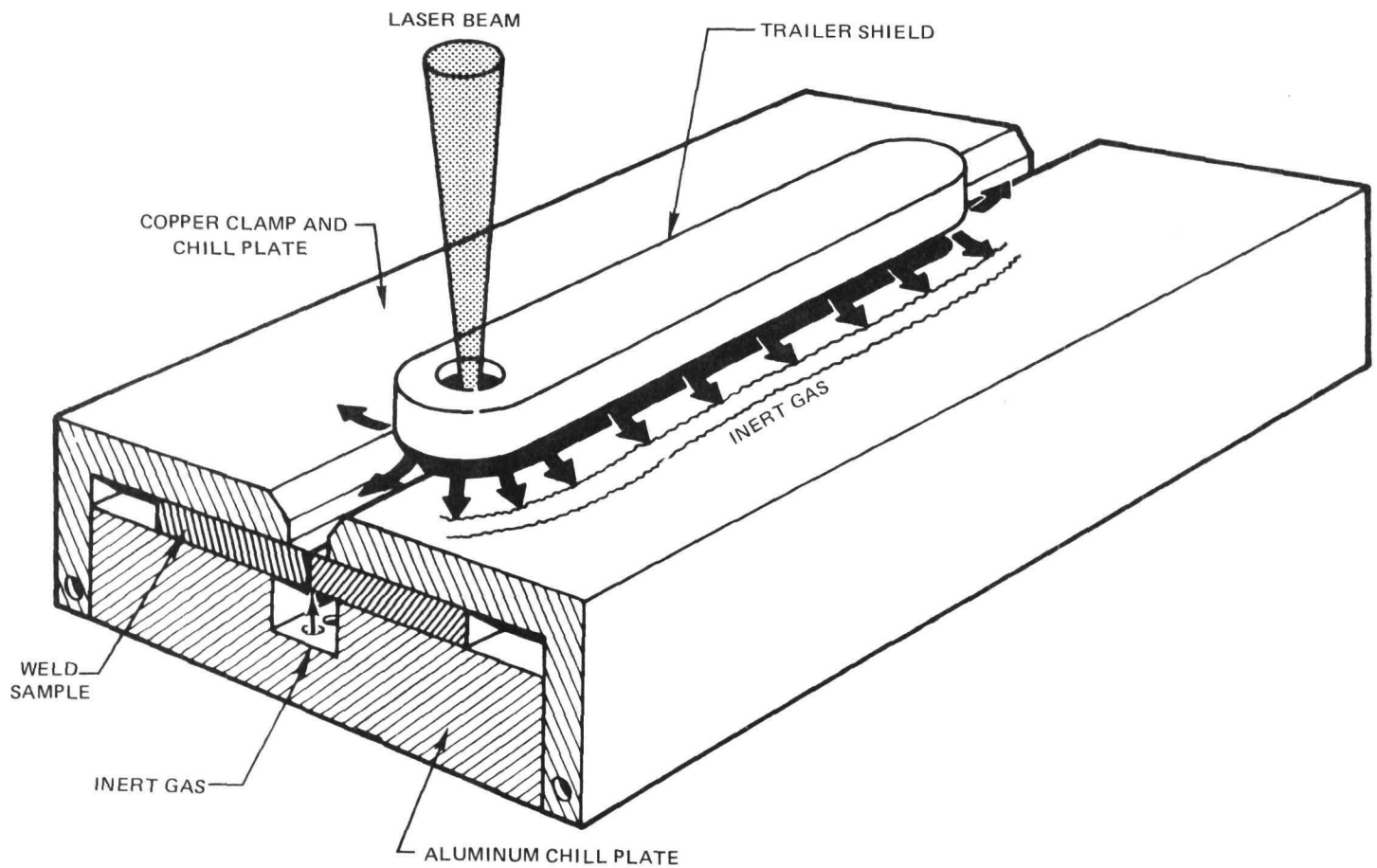

N02-134-14

FIGURE 4. RADIOGRAPHIC WELD COMPARISON

Ti–6Al–4V

0.64 cm (NOMINAL)

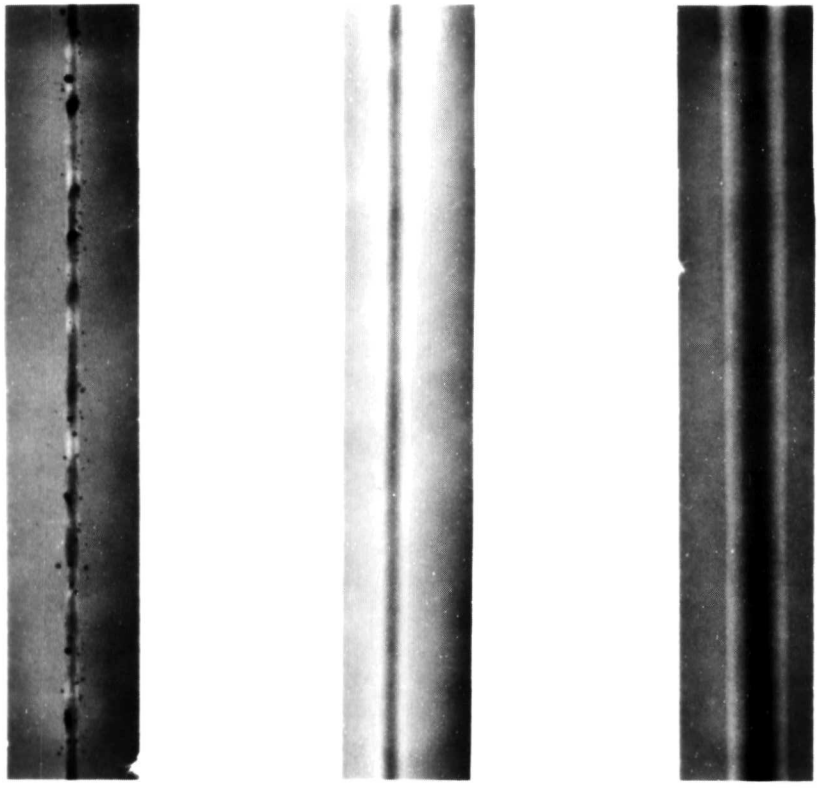

1 cm

ELECTRON BEAM
1.61 kW
1.27 cm/s

LASER
5.50 kW
2.12 cm/s

PLASMA ARC
2.10 kW
0.19 cm/s

FIGURE 5. RADIOGRAPHIC WELD COMPARISON

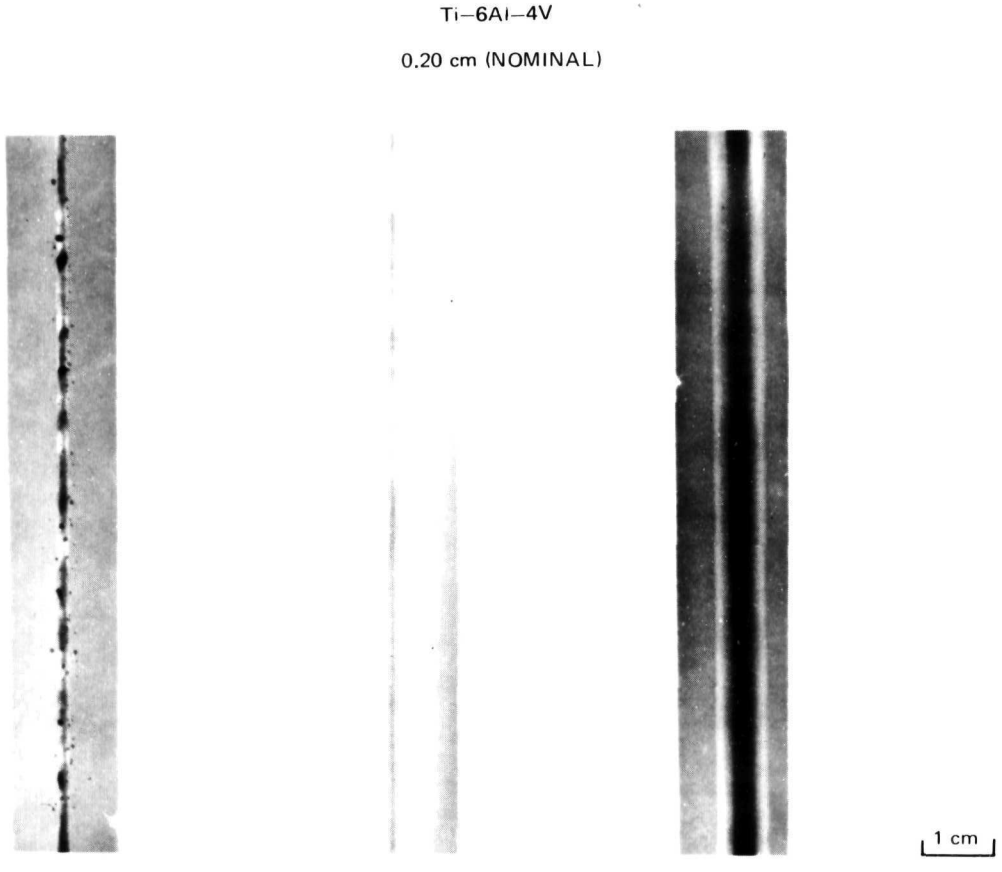

FIGURE 6. WELD MACROSTRUCTURE COMPARISON

Ti–6Al–4V

0.64 cm (NOMINAL)

6x

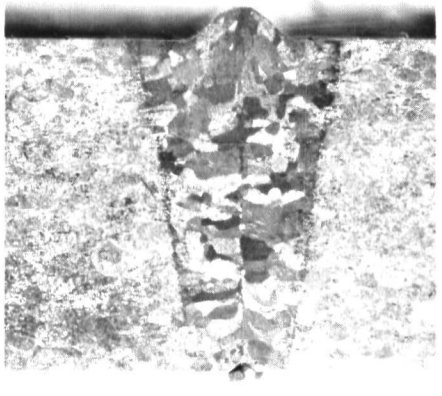

ELECTRON BEAM

1.61 kW

1.27 cm/s

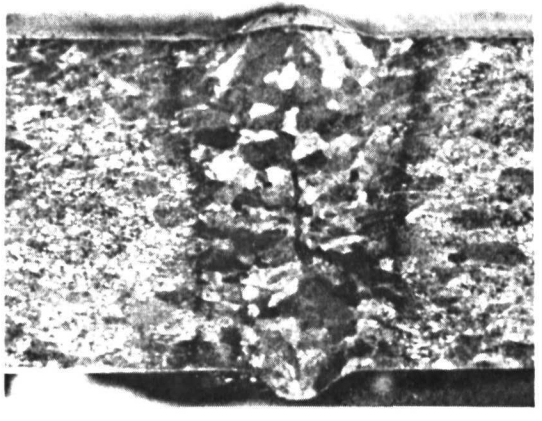

LASER

5.50 kW

2.12 cm/s

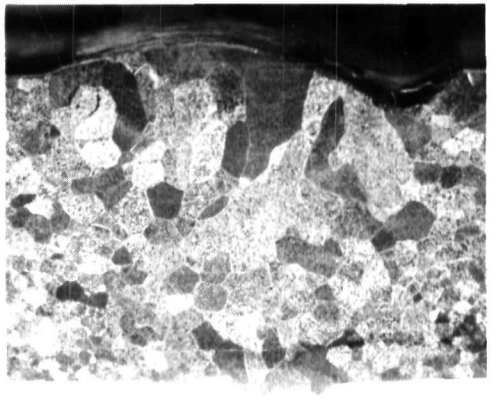

PLASMA ARC

2.20 kW

0.24 cm/s

FIGURE 7. WELD MACROSTRUCTURE COMPARISON

Ti–6Al–4V

0.20 cm (NOMINAL)

15x

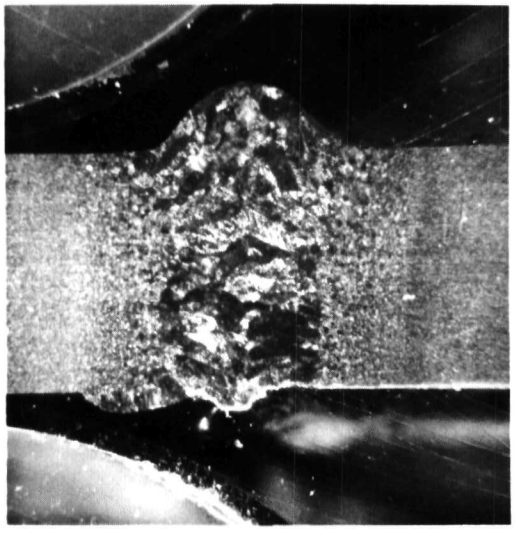

ELECTRON BEAM
1.17 kW
1.69 cm/s

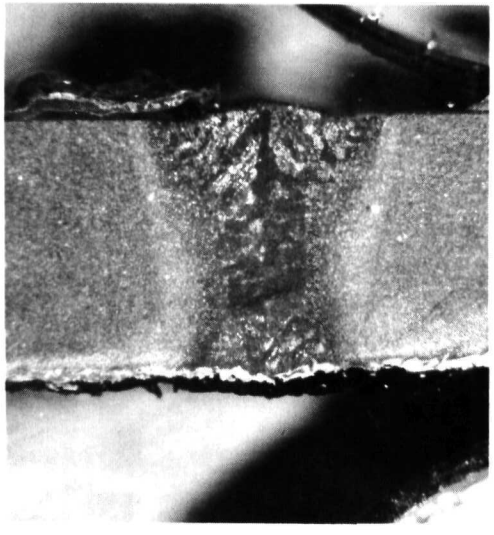

LASER
5.50 kW
5.93 cm/s

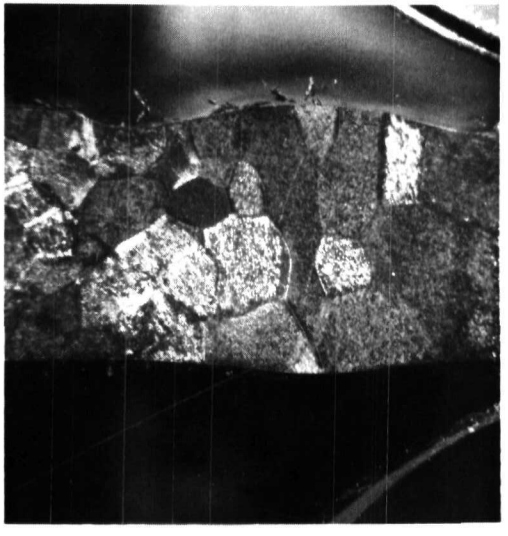

PLASMA ARC
0.50 kW
0.12 cm/s

FIGURE 8. WELD MICROSTRUCTURE COMPARISON

Ti–6Al–4V

0.64 cm (NOMINAL)

~1000x

ELECTRON BEAM

1.61 kW

1.27 cm/s

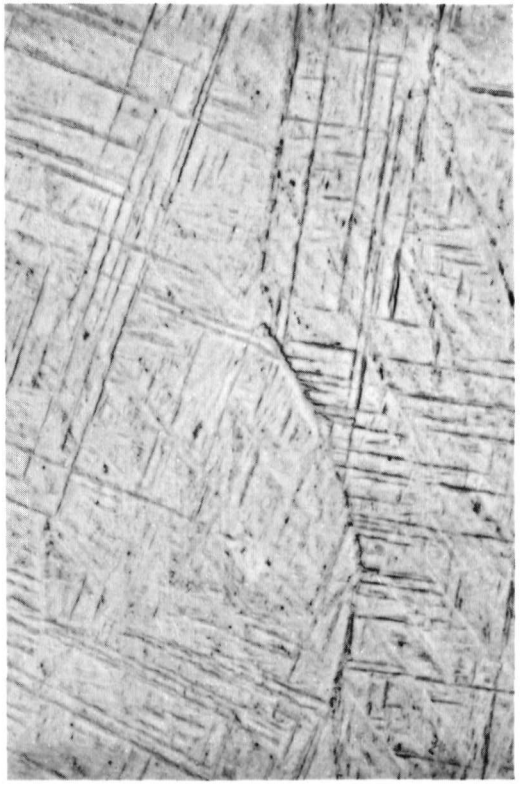

LASER

5.50 kW

2.12 cm/s

PLASMA ARC

2.10 kW

0.19 cm/s

FIGURE 9. WELD MICROSTRUCTURE COMPARISON

Ti–6Al–4V
0.20 cm (NOMINAL)
~1000x

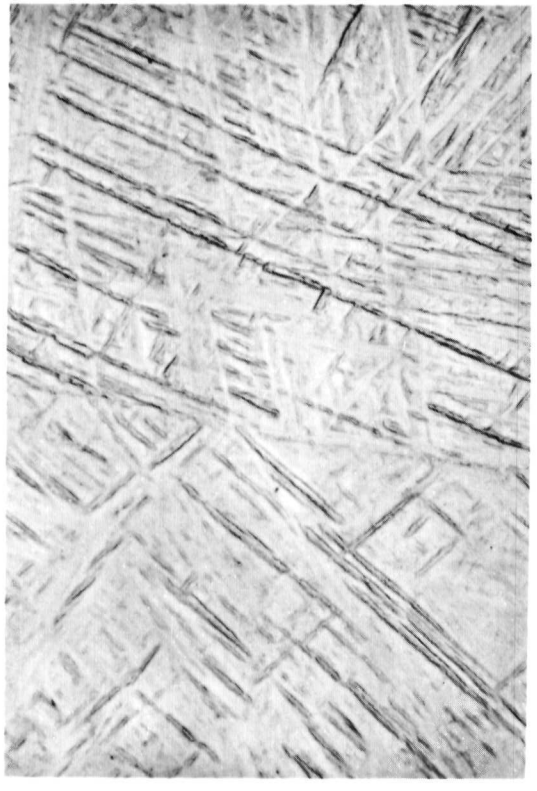

ELECTRON BEAM
1.17 kW
1.69 cm/s

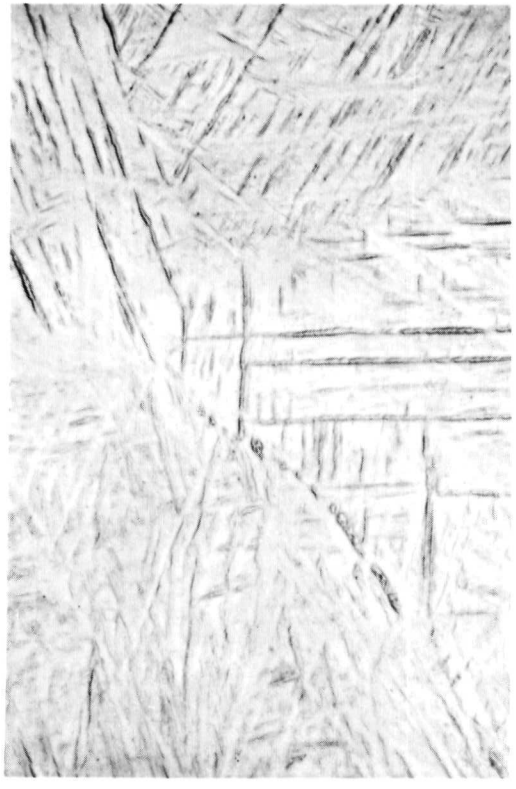

LASER
5.50 kW
5.93 cm/s

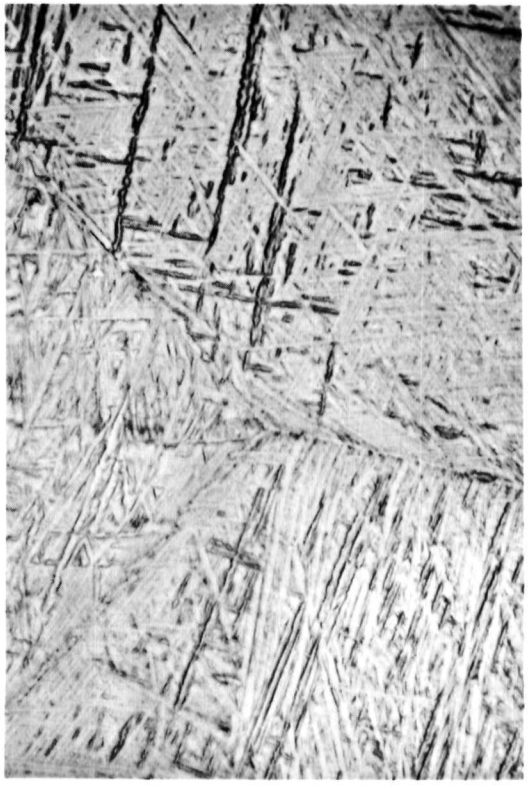

PLASMA ARC
0.76 kW
0.23 cm/s